10B
ROMS VALIDATION

LYTTELTON HARBOUR/WHAKARAUPŌ CHANNEL DEEPENING PROJECT

Pegasus Bay ROMS Hindcast Validation Report

Prepared for Lyttelton Port Company Limited (LPC)

PO Box 441, New Plymouth, New Zealand
T: 64-6-7585035 E: enquiries@metocean.co.nz

MetOcean Solutions Ltd: Report P0201-07

March 2016

Report status

Version	Date	Status	Approved by
RevA	10/03/2016	Draft for internal review	Soutelino
RevB	11/03/2016	Updated draft for internal review	McComb
RevC	12/03/2016	Draft for peer review	Beamsley
Rev0	21/09/2016	Draft for peer review	Beamsley

It is the responsibility of the reader to verify the currency of the version number of this report.

Table of Contents

List of Figures

List of Tables

1. INTRODUCTION

Lyttelton Port of Christchurch (LPC) propose deepening of the harbour shipping channel and turning basin to accommodate vessels with draughts up to 14.5 m, providing navigable depths (CD) of 16.9 m inside the entrance, grading to 17.9 m outside the heads. The estimated capital dredge volume is 11-12.5 M m^3; requiring 6-8 months effort depending on dredger. The proposed deposition site is 2.5 x 5.0 km in size and is located around 4 nautical miles from Godley Head, while the channel and turning basin extend from the port area out beyond Godley Head (Figure 1.1).

To insure that LPC can have confidence in the results from the two proposed modelling studies (plume dispersion and morphological studies), an extensive calibration and validation process of the hydrodynamic model ROMS has been undertaken and a 10-year hindcast of the current climate has been produced. With respect to the morphological modelling, it is noted that tidal and residual current transport of the dredged sediment from the proposed disposal site are expected to be minimal compared to the incident wave orbital velocity and associated asymmetric currents.

The purpose of the 10-year ROMS hindcast of Pegasus Bay is to simulate the physical ocean current environment and ultimately provide boundary conditions for higher resolution models of the sediment and particle dynamics of the study area. This report presents the ROMS model methodology (Section 2) and validation results (Section 3).

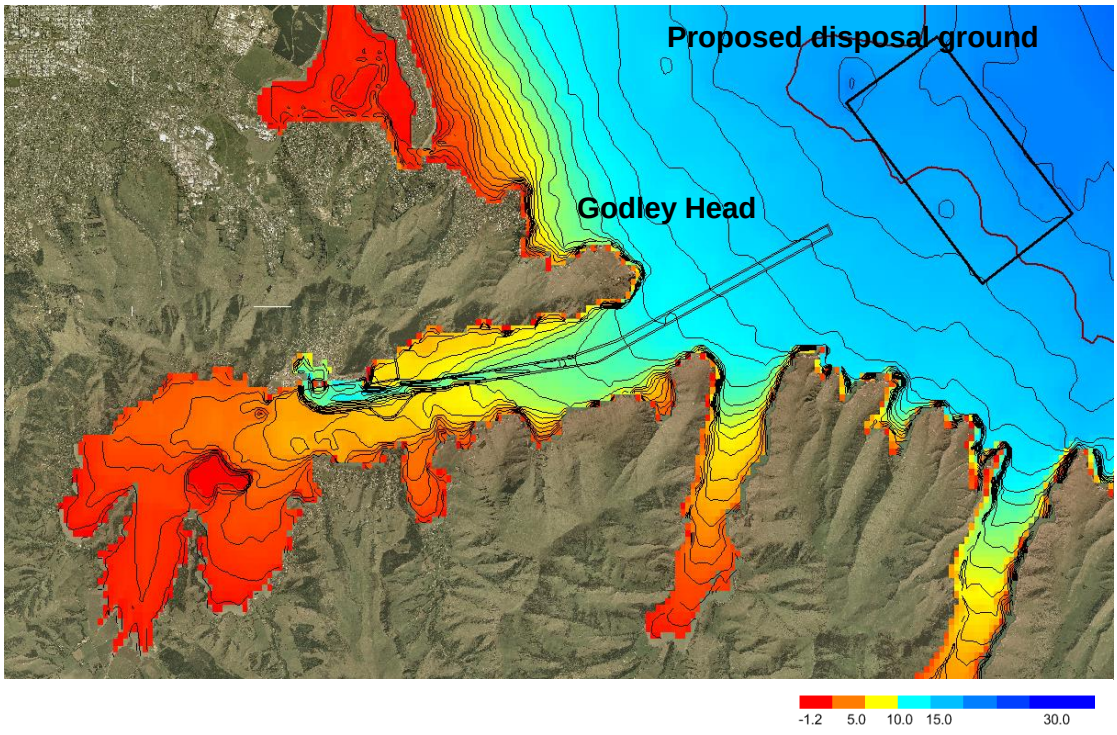

Figure 1.1 Bathymetry with footprint of the proposed deepened shipping channel and offshore capital dredging disposal ground.

2. MODEL METHODS

The primitive equation hydrodynamic model used for the hindcast setup is the Regional Ocean Modelling System (Haidvogel, et al., 2008). This tool has been used widely in the scientific and commercial consultancy communities at ocean basin, regional and coastal scales.. ROMS has curvilinear horizontal coordinate system and solves the hydrostatic, primitive equations subject to a free-surface condition. It is a state-of-the-art model widely used for regional and coastal dynamics assessment. Its terrain-following vertical coordinate system results in accurate modelling of shelf seas with variable bathymetry, allowing the vertical resolution to be inversely proportional to the local depth. Besides tidal and wind-driven currents, ROMS resolves frontal structures and baroclinic pressure gradients quite well. Vertical mixing may be resolved by different separate turbulent closure schemes, that are flexible to shallow and deep water dynamics.

2.1. Modelling strategy and domain setup

The 10-year hindcast setup is configured with a three level downscaling approach, to adequately transfer the energy gradually from larger to smaller scales, and to properly resolve the flow associated with local and remote forcing, both essential for the resultant currents in the area of interest. The open boundary conditions that are imposed to the highest level nest consists of tri-dimensional velocity, temperature, salinity and sea surface height fields derived from the 6-hourly Climate Forecast System Reanalysis CFSR and CFSv2 products (Saha et al., 2010) from the National Centers for Environmental Prediction (NCEP), which consists of a 0.5 degree global reanalysis with comprehensive data assimilation.

The larger scale ROMS nest encompasses New Zealand with 0.08 deg horizontal resolution with the goal of absorbing the basin scale circulation estimated by the CFSR global reanalysis avoiding a big parent-to-child resolution step. This domain, furthermore called NZ, is able to more adequately capture the oceanic currents around New Zealand and their variability.

An intermediate domain covers the Central West South Island (CESI) with a horizontal resolution of 0.03 deg. Besides being an essential intermediary step in resolution, the approximate 3 km applied in the CESI domain covers multiple Rossby deformation radius, allowing for more accurate representation of the quasi-geostrophic adjustment associated with the Southland Current (*SC*) magnitude and variability. Additionally, with 3 km grid spacing, the local bathymetry is more accurately captured in the important shelf-slope interface above where SC jet flows. This has shown to be crucial to provide the final nest with the right spatial-temporal variability scale of this feature, which is reported to affect Pegasus Bay circulation quite substantially.

The final local grid consists of the greater Pegasus Bay area (PEGASUS) with a 0.004 deg horizontal resolution, with the goal of resolving the mid to inner shelf and coastal currents, ultimately providing 3D flow information for the subsequent sediment transport and particle modelling. The PEGASUS domain extends far enough west and north so that possible boundary artefacts, eventual in offline nesting approaches, are far away from the main area of interest, and to properly resolve the coastally trapped waves propagating around Banks Peninsula. Additionally, these

extents aim to allow the model to capture the literature-reported flow injections from the *SC* in the form of topographically-forced anti-cyclonic eddies.

The 3D flow and mass fields are transferred from the top level domains to the smaller domains by the offline one-way nesting technique. CFSR 3D fields are fed into the NZ scaled ROMS domain at a 6-hourly interval and NZ-to-CESI and CESI-to-PEGASUS in a 3-hourly interval. ROMS NZ and CESI domains do not include tides, since they are deeper ocean setups and minimally affected by them. Moreover, the tides impose rigorous time step constrains, which would impact the run durations substantially.

All domains are submitted to spin-up phases prior to the 10-year hindcast period and/or calibrations period, to allow the adjustment of the coarser initial conditions to higher resolution and its more detailed topography. The spin-up times are hierarchically established according to the main scales that each one is supposed to resolve. This information and all other relevant information for each of the hydrodynamic model domains considered for this study are summarised in **Error! Reference source not ound.** The model bathymetry for each of the ROMS domains was derived from electronic navigation charts or field data whenever available. For the deep areas of the NZ domain, GEBCO data was merged in.

Table 2.1 ROMS domains relevant characteristics.

Model Settings	**NZ**	**CESI**	**PEGASUS**
Horizontal resolution [deg]	0.08	0.03	0.004
Vertical S-layers	24	23	18
Tidal forcing	No	No	Yes
θs, θb stretching parameters	5 ; 0.4	5 ; 2	5 ; 5
Baroclinic time step [s]	120	100	40
Minimum depth [m]	20	10	5
Atmospheric forcing	WRF 12 km	WRF 12 km	WRF 12 km
Spin up time	5 years +	1 year	3 months

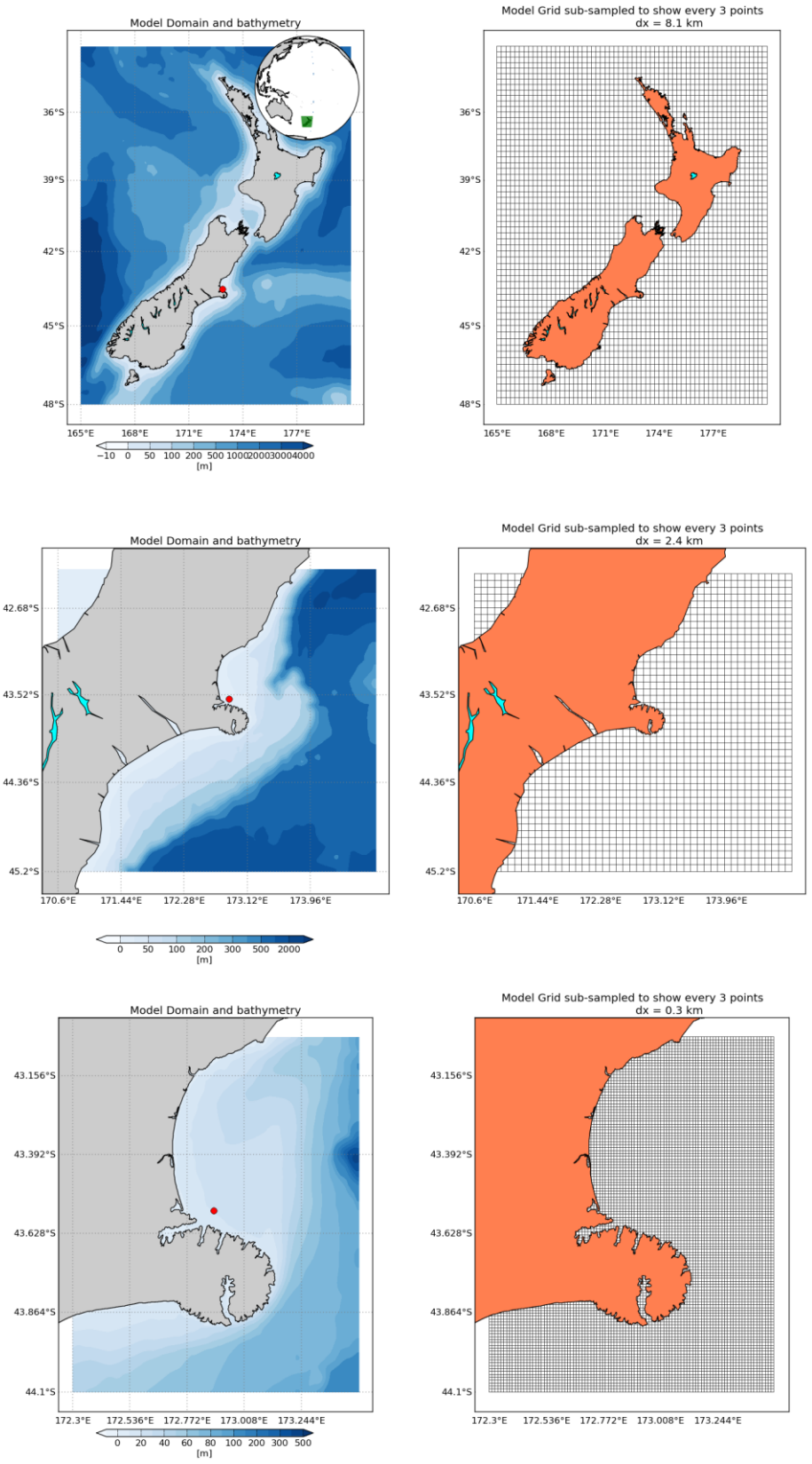

Figure 2.1 Hydrodynamical hindcast downscaling approach with ROMS. Upper panel shows the NZ 0.08 deg domain, middle panel shows the intermediate 0.03 deg CESI domain and lower panel shows the 0.003 deg PEGASUS domain. The right panel grids are showing every other 3 grid points, to allow easier graphical interpretation. Land mask is applied to the NW corner of CESI grid.

2.2. Atmospheric forcing

MetOcean Solutions maintains an up-to-date 10-15 km resolution New Zealand atmospheric reanalysis from 1979-2014 produced with the WRF model and deriving boundary conditions from the same global CFSR product used to initialize and force ROMS NZ. This leap of resolution from the 35 km available from CFSR adds accuracy and variability to the atmospheric fields that force ROMS, especially around Banks Peninsula area, where topography is known to substantially change the large scale wind patterns and its local response. WRF reanalysis prognostic variables such as winds, atmospheric pressure, relative humidity, surface temperature, long and short wave radiation and precipitation rate are used at hourly intervals to provide air-sea fluxes to force ROMS in all domains, using a *bulk flux* parameterization (Fairall, et al., 2003).

2.3. Tidal forcing

The widely used tidal constituents sourced to force regional and coastal domains in hydrodynamic models - the Oregon State University Tidal Inverse Solution (OTIS, Egbert and Erofeeva, 2002) – is rather course for direct use in New Zealand coastal domains. Therefore, tidal constituents for the New Zealand domains benefit from the harmonic analysis of a long term 2D POM tidal simulation with 5 km horizontal resolution at the same grid coverage presented in the upper panel of Figure 2.1. This POM domain is forced at the open boundaries by tidal elevation and current harmonic constituents derived from OTIS Pacific Ocean solution, and has shown improved validation results in many areas when compared to OTIS. The PEGASUS ROMS domain is than forced at the open boundaries by elevations and currents constituents derived from this POM 2D source.

2.4. Open boundary conditions

High frequency (6-hourly for NZ and 3-hourly for CESI and PEGASUS) open boundary 3D mass and velocity fields are considered for all domains. Passive/active prescriptions are applied for all 3D variables at the open boundaries, where a radiation scheme is applied when outflows are estimated by ROMS algorithms. When/where inflow is detected, a nudging condition is applied, allowing the penetration of 3D transports and T-S from the external sources, a key setting to guarantee the SC contributions to the smaller scales. To account for the fast propagating tidal oscillations, 2D velocities and surface elevations are treated with *Flather* and *Chapman* schemes, respectively.

2.5. Model calibration process

Model calibration and validation are the primary processes for quantifying and building credibility in numerical models. Contemporary numerical primitive equations models nowadays are quite accurate in resolving the equations of motion and sub-grid scale parameterizations. Initial, forcing and boundary conditions are usually the determining factors to how accurate a hindcast is. Along with numerical diagnosis such as checking kinetic energy equilibrium and trends in the 3D fields, testing the model against observations is key to show how reliable the numerical solutions are.

Through comprehensive testing of model parameters such as sub-grid scale parameterizations, forcing sources and grid settings such as open boundary locations, spatial resolution and downscaling rate between parent and child grids, the model was calibrated until it reached the best matching against measurements in the area of interest. This process focused on best representing the total depth-averaged currents, with particular focus on the sub-inertial band, i.e. with periods higher than 40 hours.

2.6. Measured data

The measurements available for model calibration/validation consists of 7 current meters moorings, of which 6 came from an ADP and 1 from an ADCP. Geographical locations and details about the instruments are shown in Figure 2.2 and Table 2.1. The measurements at all sites consists of post-processed depth-averaged total velocities at 30 minute intervals For each location, ROMS virtual stations were pre-set and saved at the same time interval to optimize calibration and validation procedures. Since the measurement campaigns were sparse in time and the model requires a certain amount of spin up prior to the measurement period, it is not practical to consider all instruments for the calibration, and so ADP-1, ADP-2 and SB were chosen.

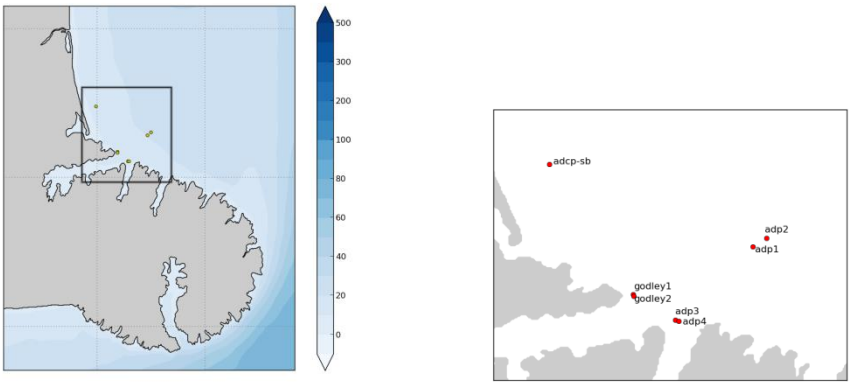

Figure 2.2 Location of the available measurements for model calibration/validation.

Table 2.2 Summary of available data.

Station	Lat	Lon	Start Date	End Date	No Days
ADP-1	-43.561	172.882	26/10/2007	12/12/2007	47
ADP-2	-43.557	172.8901	21/02/2008	12/03/2008	20
ADP-3	-43.602	172.8396	20/03/2008	5/06/2008	77
ADP-4	-43.603	172.8418	5/06/2008	13/08/2008	69
Godley1	-43.589	172.8168	2/05/2009	3/06/2009	32
Godley2	-43.588	172.8165	2/10/2009	4/11/2009	33
SB	-43.516	172.7700	29/01/1999	11/04/1999	72

3. VALIDATION RESULTS

3.1. Qualitative validation

As a first proxy of the modelling performance, monthly mean depth-averaged flow fields are presented (Figs. 3.1-3.2) discussed. The goal here is to evaluate the models' ability to correctly represent the main features of the regional circulation.

The main large scale features are successfully represented by the model. The SC flowing to NE and its cyclonic meandering as part of the retroflection towards open-ocean off Banks Peninsula in the subtropical convergence area can be clearly identified. The presence of an enduring and large anti-cyclonic feature in Pegasus Bay is evident, indicating the model skill to represent this particularly important forcing mechanism to the local shelf flow in the area.

The zoomed in view on Figure 3.3 shows the benefit of the high resolution ROMS grid (PEGASUS) to better resolve the spatial structure of the Pegasus Bay anticyclone, as well as an adequate prescription of the open boundary conditions, which are allowing the dynamics from CESI domain to correctly influence PEGASUS. Once again, the expected literature-described pattern is well captured by the model. At a local level (Fig. 3.4) note the prevalence of flows directed to the SE at the proposed dump ground area, which is well-captured and present in all months studies here.

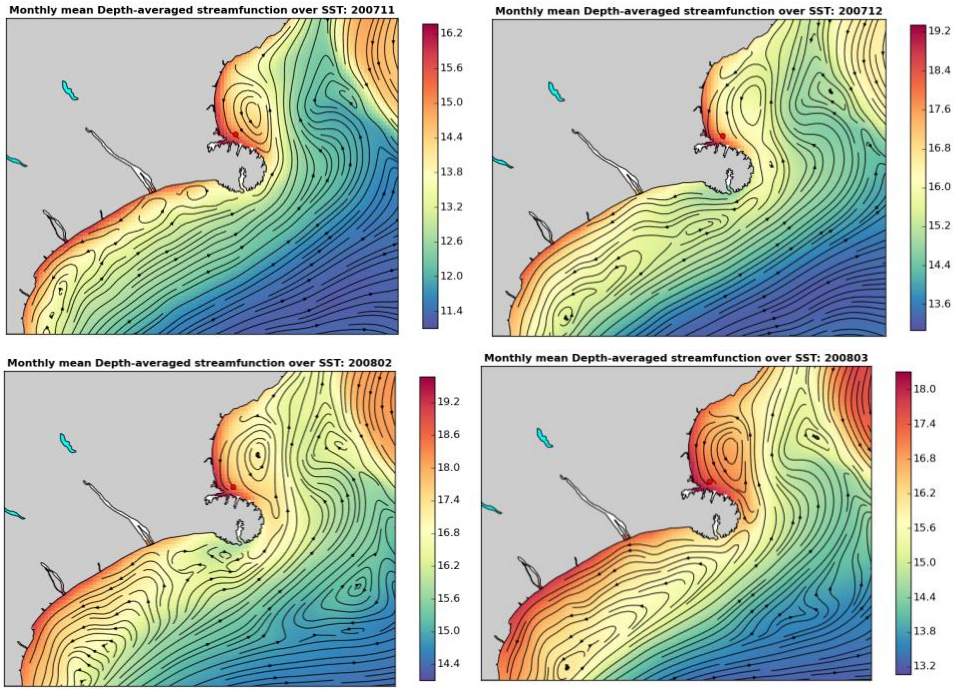

Figure 3.1 Monthly mean depth-averaged stream function maps for Nov-Dec 2007 and Feb-Mar 2008 for the CESI ROMS domain. These four months corresponds roughly to the periods of the ADP-1 and ADP-2 campaigns. The red dot represents the ADP-1 location.

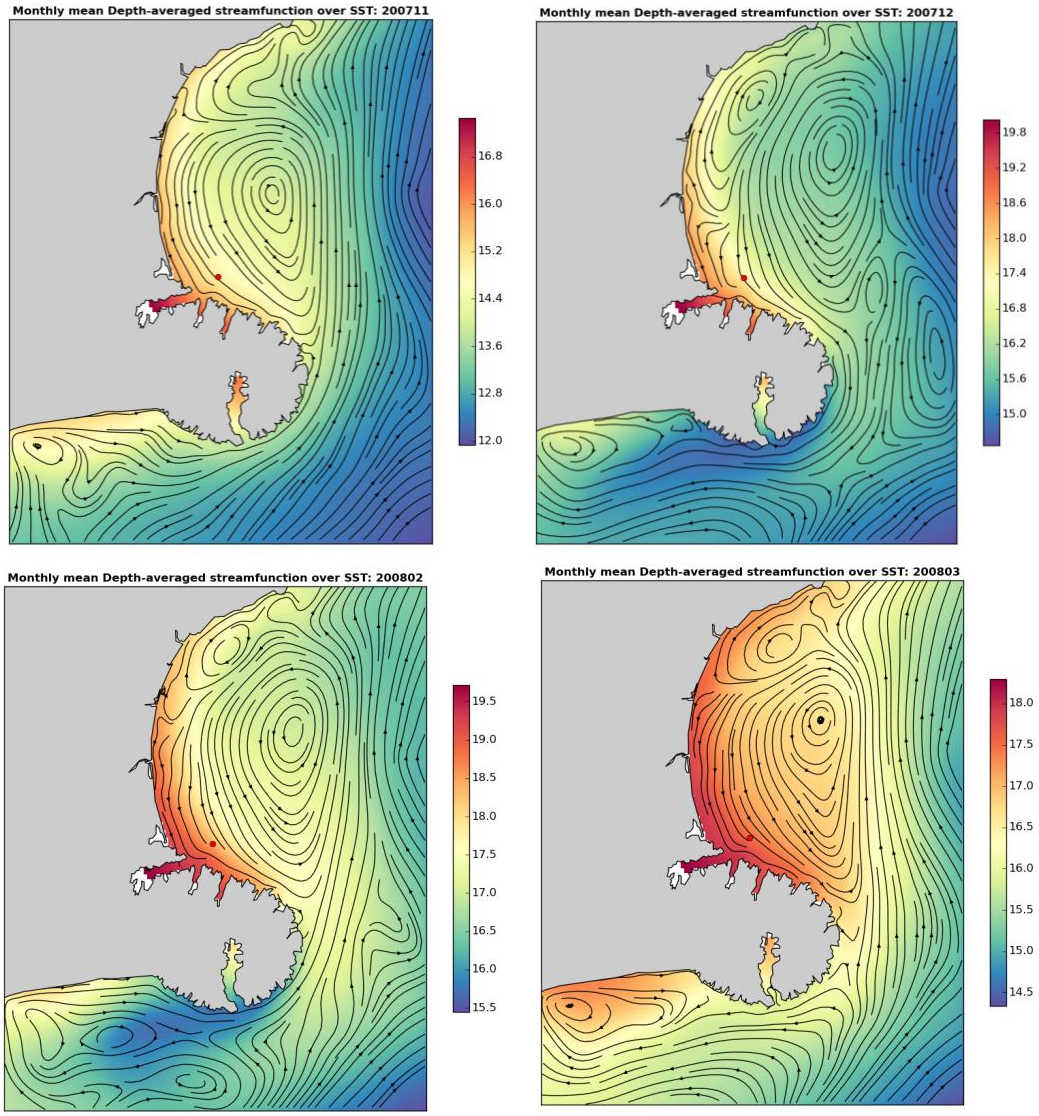

Figure 3.2 Monthly mean depth-averaged stream function maps for Nov-Dec 2007 and Feb-Mar 2008 for the PEGASUS ROMS domain. These four months corresponds roughly to the periods of the ADP-1 and ADP-2 campaigns. The red dot represents the ADP-1 location.

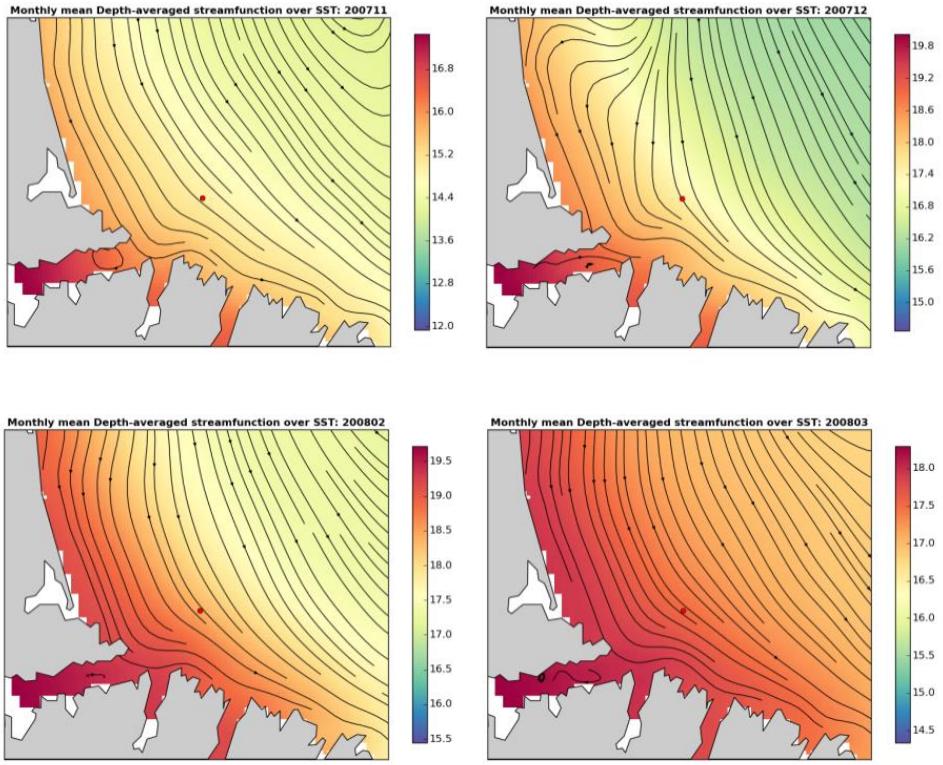

Figure 3.3 Monthly mean depth-averaged stream function maps for Nov-Dec 2007 and Feb-Mar 2008 for the PEGASUS ROMS domain focusing in the dump ground area. These four months corresponds roughly to the periods of the ADP-1 and ADP-2 campaigns. The red dot represents the ADP-1 location.

3.2. Quantitative validation

Total currents from the measured and modelled sources at ADP-1, ADP-2 and SB are presented as time series on Figure 3.4, and quantile-quantile plots on Figure 3.5 and velocity vector scatter plots on Figure 3.6. Summary validation statistics are provided in Table 3.1.

This nearshore region is characterized by a relatively weak overall flow regime and a tidal current regime that reaches around 10 cm.s^{-1} amplitude and shows only a small spring-neap modulation. In general, the modelled total currents have reasonable agreement with the co-temporal measured values. Departures from tidal flows are noted in both modelled and observed data, which is discussed later when the sub inertial conditions are analysed. In general, the ROMS hindcast well represents the main variability axis, which is along-shelf in this region. However, at times the model does seem to under estimate the cross-shelf component. Both model and observed data agree with a mean south-eastward flow, which is expected as the local response to recurrent SC anti-cyclonic eddy injecting energy into Pegasus Bay.

While tidal currents have an important diffusive effect on the movement of suspended sediments, it is the residual currents that are the primary driver for net transportation. Accordingly, model performance was evaluated against the measured data for aspects of the non-tidal sub-inertial flows. A

40-hour low-pass Butterworth filter was applied to both the modelled and the measured velocities, which were both introduced with a 30-minute interval as an input. The results are shown in Figures 3.6-3.8, and summary validation statistics are provided in Table 3.1.

It is notable that these residual (i.e. non-tidal) flows are typically weak and often fall into the noise level for reliable instrument and model resolution. As with the total flow regime, these velocities are mostly oriented in the along-shelf direction, in a pattern that is well captured by the model. Once again, it is noted that the model under-estimates the cross-shelf residual flows, but the magnitudes are low and therefore not significant from a sediment entrainment perspective. There may be some slight bias to plume advection or transport of suspended material under wave-stirring.

The model performs remarkably well for the ADP-2 location, with almost all events being reproduced, albeit some slightly overestimated and some slightly underestimated. The residual current events are likely related either to wind-driven local and remote shelf dynamics or local response to *SC* variability, but these are shown to have a relatively small local signal, and therefore absolute differences between model and measurements should be considered cautiously. Overall, the model seems to slightly underestimate the residual currents, but the BIAS for ADP-1 and ADP-2 (less than 2 $cm.s^{-1}$, as Table 3.1) is low, with BIAS slightly higher for SB location (4 $cm.s^{-1}$). Some events are not reproduced by the model, especially in ADP-1 and SB.

Regardless of the discrepancies, it is interesting to note the differences between ADP-1 and ADP-2 validations. ADP-2 shows much better agreement between model and measurements than ADP-1, although they are only about 500 m apart and very close time-wise. Small differences in instrument calibration, installation and measurement campaign details (not exposed to the modeller) could possibly explain this. At SB however, the model performs much worse, with significant underestimation of the residual currents. Information on that meter and the type of mooring was not available so comment cannot be made regarding the data quality.

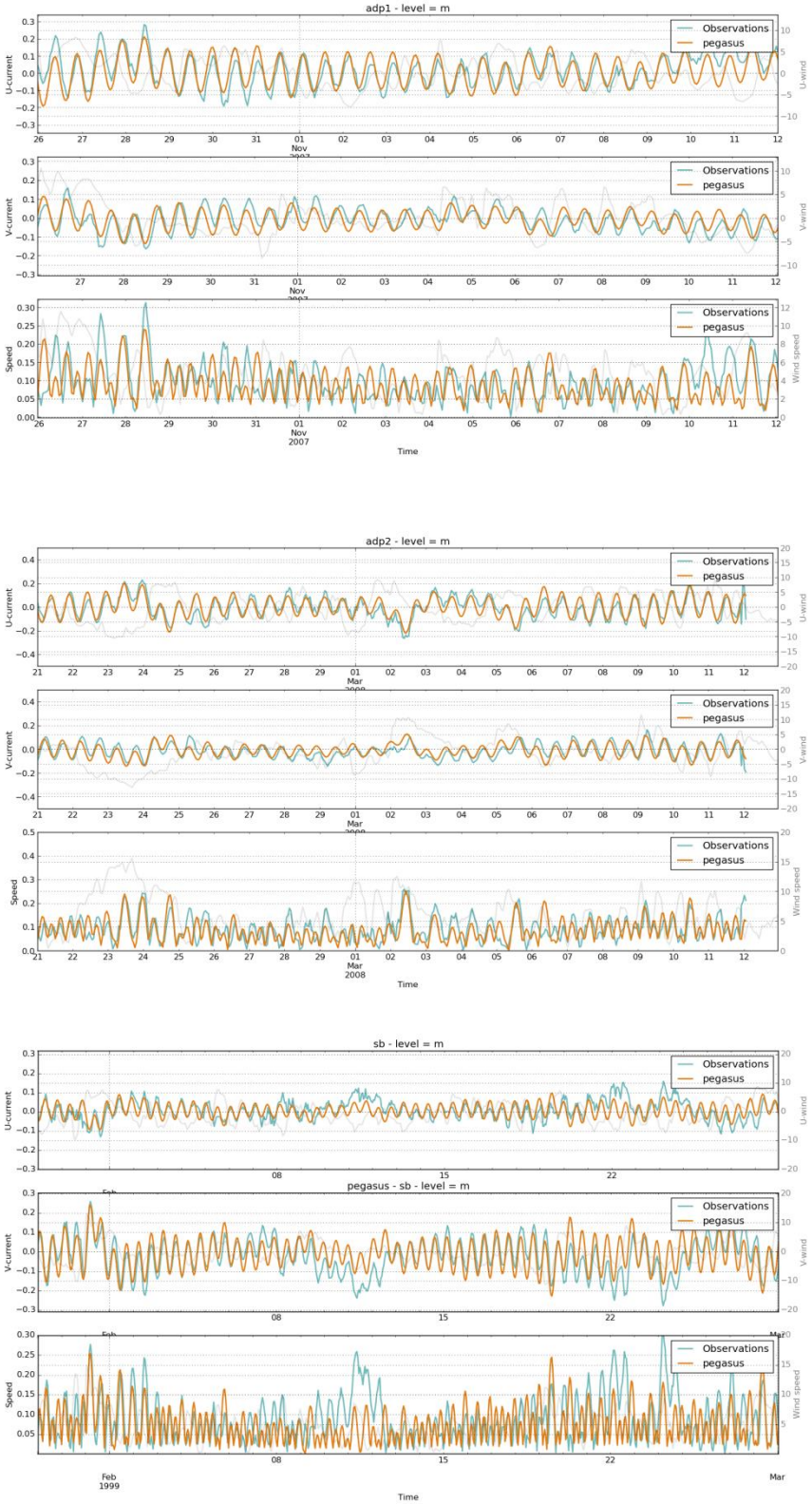

Figure 3.4 Total velocities time series at ADP-1, ADP-2 and SB. ROMS PEGASUS shown in orange, observations in green. The grey curve represents the wind used to force the model, to help interpretation of significant events. Only the beginning of ADP-1 and SB series is shown to better allow inspection of tidal signal amplitude and phase match.

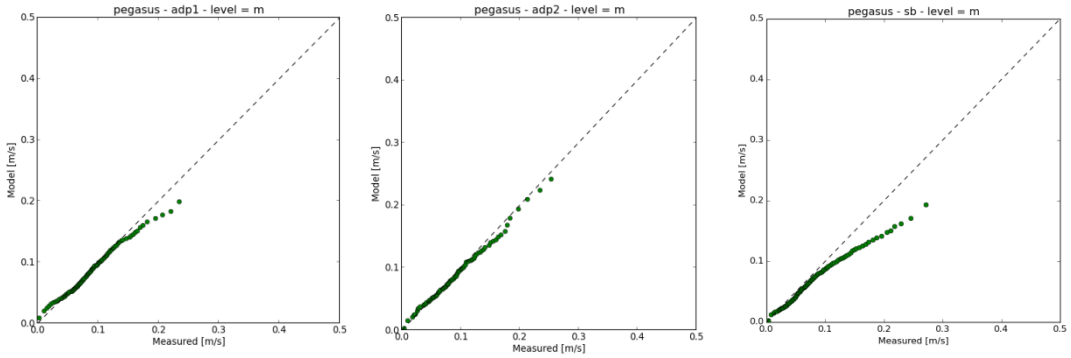

Figure 3.5 Quantile-quantile plot for total current speeds at ADP-1, ADP-2 and SB.

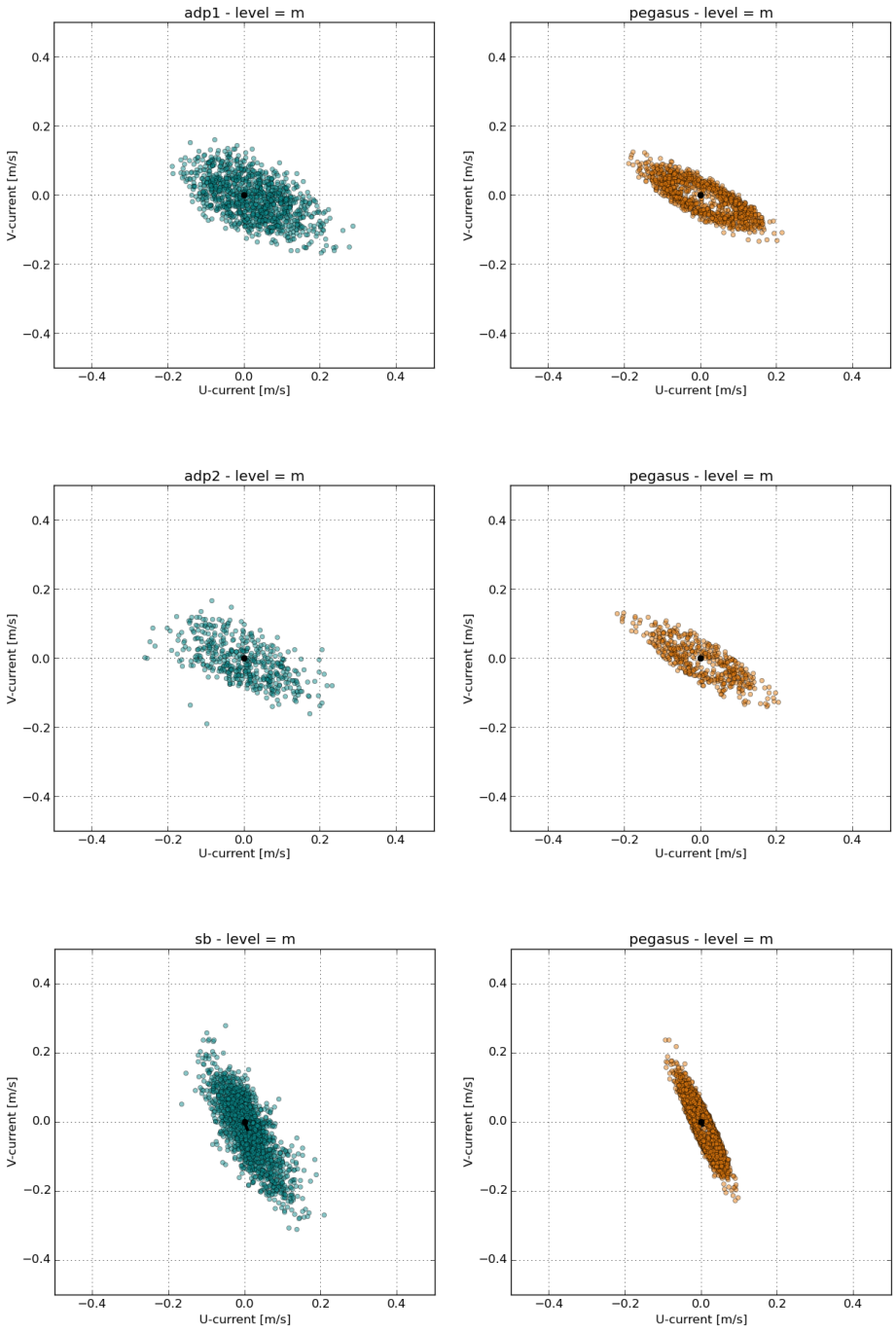

Figure 3.6 Velocity vector scatter plot for total velocities at ADP-1, ADP-2 and SB.

Figure 3.7 Residual velocities time series at ADP-1, ADP-2 and SB. ROMS PEGASUS shown in orange, observations in green.

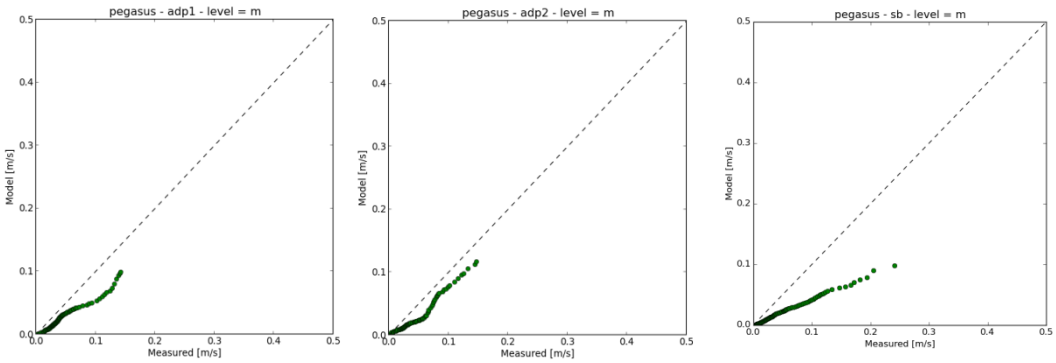

Figure 3.8 Quantile-quantile plot for residual current speeds at ADP-1, ADP-2 and SB.

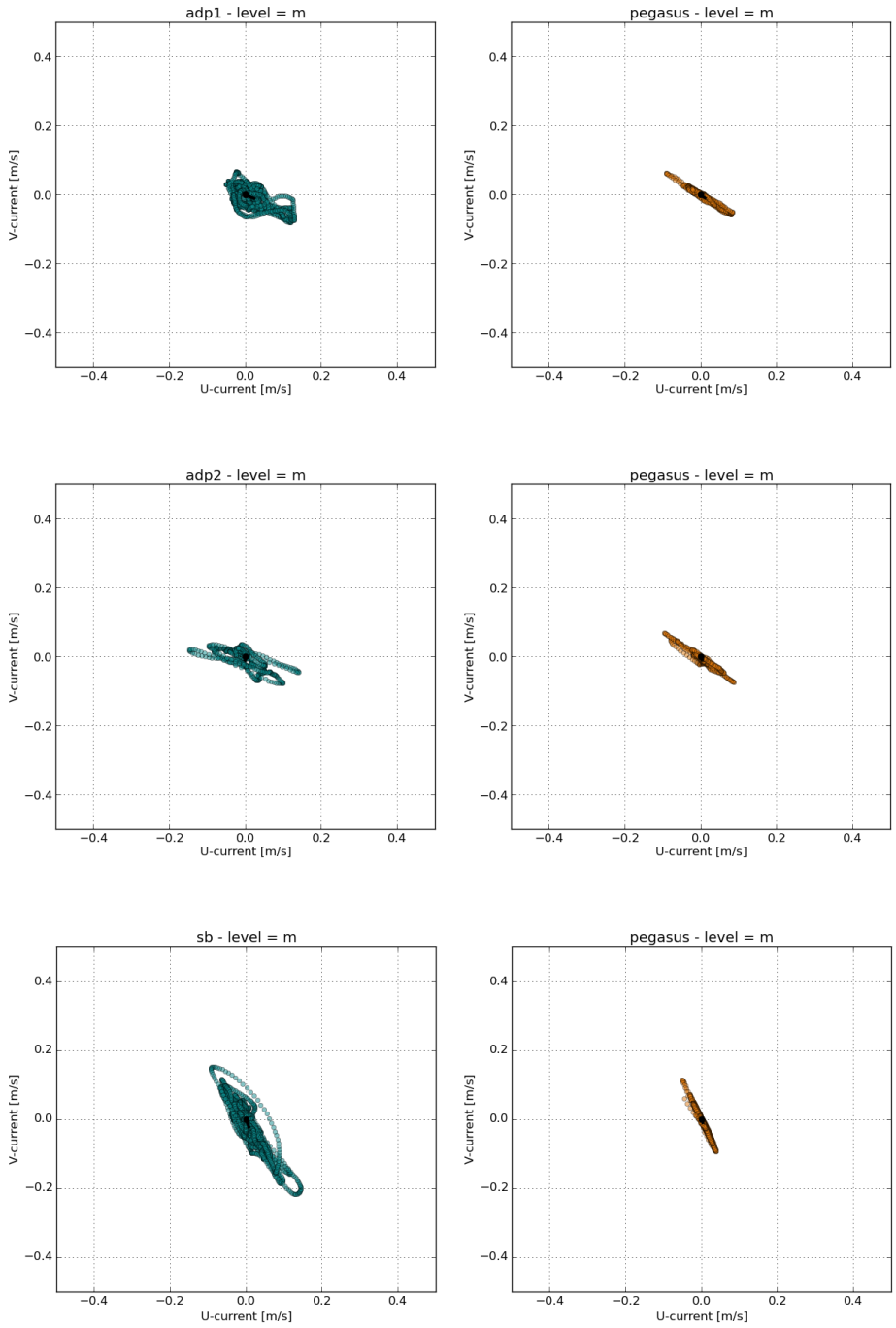

Figure 3.9 Velocity vector scatter plot for residual velocities at ADP-1, ADP-2 and SB.

Table 3.1 Summary validation statistics for ADP-1, ADP-2 and SB locations. MAE is the mean absolute error while RMSE is the root mean square error.

	Total velocity (m/s)			**Residual velocity (m/s)**		
	ADP-1	**ADP-2**	**SB**	**ADP-1**	**ADP-2**	**SB**
BIAS	-0.005	-0.004	-0.015	-0.019	-0.019	-0.036
MAE	0.037	0.035	0.048	0.027	0.028	0.045
RMSE	0.047	0.044	0.062	0.036	0.035	0.062

4. DISCUSSION

An aspect that is worth noting is that terrain-following vertical coordinate models such as ROMS, despite showing many advantages to resolve shelf and coastal dynamics, require a degree of pre-processing of the realistic bathymetry in order to minimize baroclinic pressure gradient truncation errors caused by the displacement between the sigma levels and the local horizontal axis in the presence of steep topographic gradients. In other words, in order to preserve the first order dynamics within a sensible error-free computation, the real bathymetry needs to be slightly modified at certain locations, which can lead to subtle spatial differences in the flow paths. Skipping that step is not recommended by the ROMS developing community, since it may introduce spurious velocities driven by pressure gradient errors. This is particularly critical for this application due to the nature of *SC* forcing, which has an important baroclinic geostrophic component to it. This could explain some of the underestimation noted in ROMS comparisons with measurements, especially at SB site. Small differences in bathymetric slopes and absolute depth in the shelf break can steer the flow differently into the mid and inner shelves.

While the comparison of model and measurements in a single point is all there is available to test if the model results are reproducing realistic flows, it holds several limitations with regards to prove the model ability to represent the flow spatially, which is what ultimately determine the fate of sediments in the region. Spatial variability in the wind field and remote dynamics influence to local circulation can also lead to slightly different flow patterns in a single site location, but this may or may not reflect the model ability to capture the realistic flows in a spatial sense.

With that in mind, an event-based analysis was conducted to better understand the spatial residual flow snapshots at periods where the model had a good performance and at periods that model didn't quite captured what the measurements indicate. Focus is given to the particular SE flow events where there was potential contribution from the *SC*.

The SE flow event of October 28-29, for instance, was fairly well captured by the model (Fig. 4.1). Examination of the spatial aspects of the flow and how it correlates to different forcing mechanisms (see Figs. 4.2 – 4.3) is very informative. Starting with the larger scale patterns, it is noted that little has changed in the SC flow structure from October 28 to October 29. The *SC* jet may be interpreted by the relatively wide band of flow going towards the NE, roughly where water temperature is less than 9 deg C. As one would expect, it's a very wide jet structure when compared to flow features in the coastal area, and it obviously varies in much longer time scales than the two days shown here. What changes clearly between October 28th and 29th is the wind-driven flow over the continental shelf. The event is characterized by three days of strong SW wind, shown in the small lower panels of the figures. The October 28th daily residual flow snapshot occurs while the strong SW is still blowing with substantial strength (around 10 m.s^{-1}, as seen in the red emphasized vector). As expected, local currents and sub-inertial geostrophic adjustment would be already in place by this time scale, and we can see relatively strong flows to the NW around the entire continental shelf of the model domain. These NE-oriented geostrophic coastal jet bands over the Banks Peninsula with no signs of anti-cyclonic eddy formation and leaves the proposed dump ground shadowed and with relatively weak flow, which probably corresponds to the

moment where ROMS zonal and meridional flow components time series are crossing the zero line The described pattern for October 28th can be seen even more clearly on Figure 4.2 and 4.3.

By October 29th, a substantial relaxation of the SW wind is noted, with slight reversal to NE. While most of the continental shelf flow at the PEGASUS domain seems to vanish at this point, the Pegasus Bay exhibits a clear anti-cyclonic eddy. What seems to be happening in this two day scenario is that there is a background large scale *SC* flow and a shelf anti-cyclonic flow in Pegasus Bay as a consequence, and this eddy is masked out by the action of the strong SW wind-driven flow from days prior to October 28th and October 28th itself, but revealed by the absence of substantial wind in October 29th. This strongly indicates that the variability that is responsible for that residual displacement in the current at ADP-1 is caused by the local wind rather than a *SC* fluctuation.

In fact, a closer look at the upper panel of Figure 4.2 suggests a correlation between the strong westerly winds and weak currents at the proposed dump ground, corroborating the potential that there is a background eddy that reveals itself in the absence of wind and is masked when there is an opposing wind. Independent of the dynamics behind the local flow response to these two forcing mechanisms, if focus is given to the proposed dump ground area (Fig. 4.3) it may be noted that there is a gradual intensification of the SE flow as we move from areas closer to the coast to areas offshore. A slight variation of any of these factors might as well have caused this event to not be as greatly captured as it was, but in this case it was. The understanding of any bias observed between ROMS and measurements in a particular event like this is very limited by the punctual nature of the measurements, but regardless, the model has shown satisfactory skill to capture this event in the spatial and dynamical forcing factors.

Considering a poorly reproduced event (Figs. 4.4-4.6) from November 11-12th, one may draw similar conclusions. First, it's very interesting to note that the spatial structure, location and magnitude of the *SC* appears to remain intact compared to the snapshots in Figure 4.1, further indicating that this feature is driven by large scale mechanisms and changes in a much slower time scale. The same can be said for the westward meander that detaches from it offshore mid Pegasus Bay and finally folds over and thereby becomes the typical anti-cyclonic flow feature. Here, the observation that the model failed to represent the event in terms of magnitude is likely related to synoptic wind variability than to variability in the *SC* flow. The *SC* variability should be considered on much longer time scales than the ones that these SE current bursts occur and remain active. Once again, on Figure 4.5 on November 11th there seems to be a southward decrease of the meridional current magnitude at Pegasus Bay, which might explain the delay of the model in capturing this particular SE event (as can be noted also in Fig. 4.1). On November 12, the flow seems to be more accelerated due to the start of a NE wind in the region. There is once again a clear spatial variability of the flow in the surroundings of the proposed dump ground, which might indicate that this poor reproduction by the model is an artefact of the combined variations of all the forcing mechanisms and its non-linear interactions, which can randomly play in favour or against the validation result in that particular point of a much broader area of interest where sediment transport is to be studied.

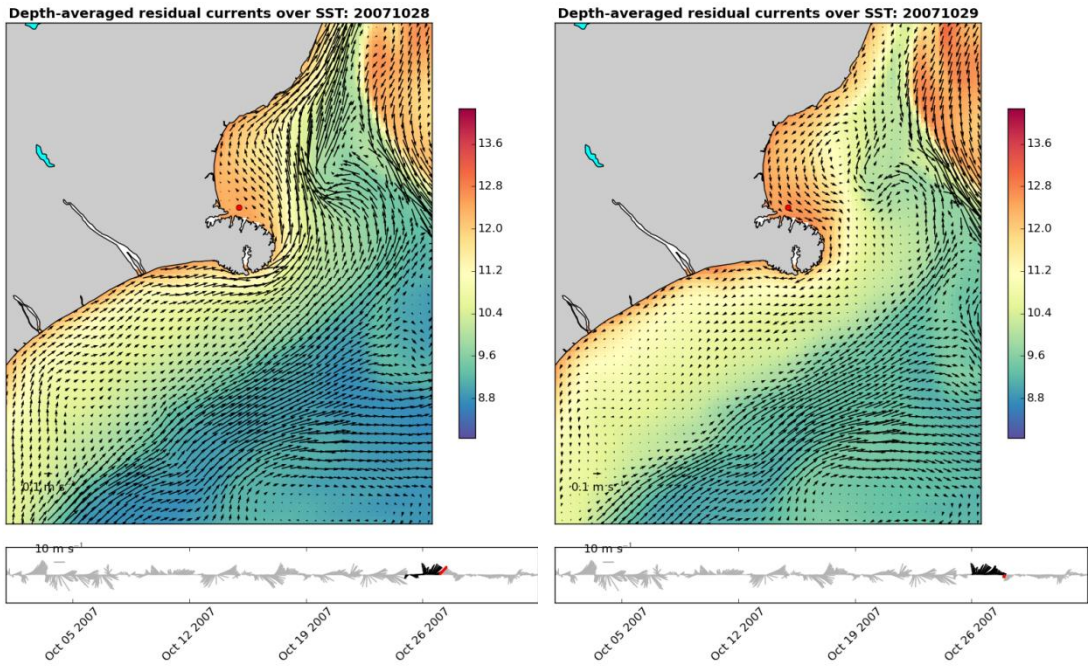

Figure 4.1 CESI ROMS domain residual depth-averaged flow daily snapshots for October 28 and 29, 2007, coinciding with ADP-1 measurements. The red dot represents the ADP-1 site location. The small lower panels show the time series of the wind used to force the model during that particular month, extracted at the center of Pegasus Bay. The stronger black wind vectors emphasise the wind during two days prior to the flow snapshot, and the strong red vectors corresponds to the day of the flow snapshot.

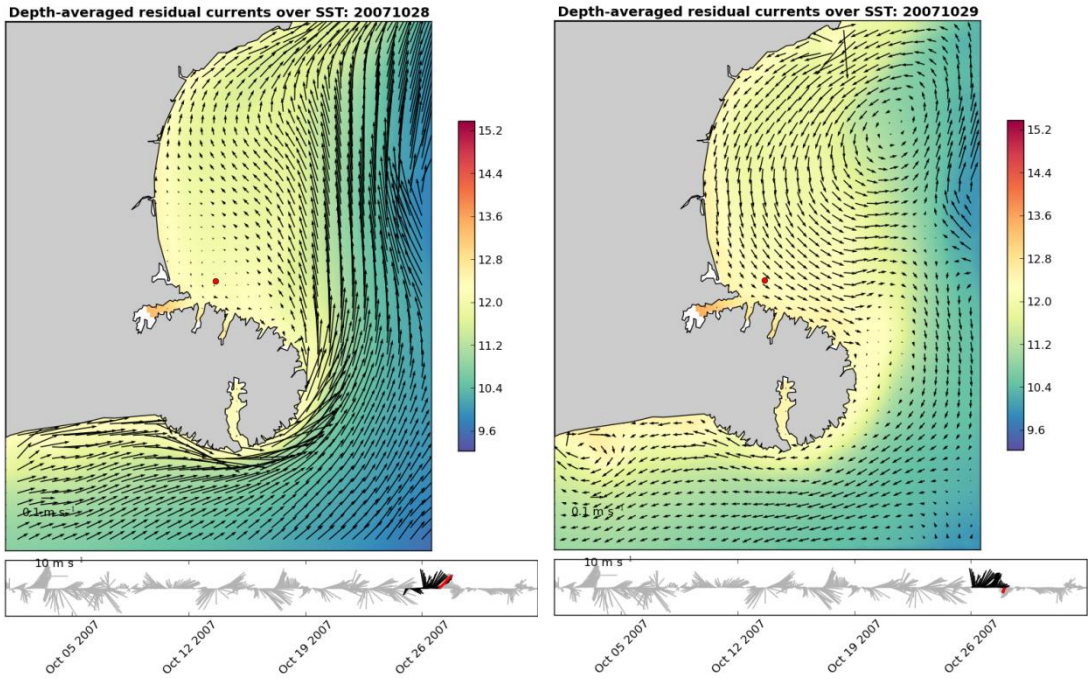

Figure 4.2 PEGASUS ROMS domain residual depth-averaged flow daily snapshots for October 28 and 29, 2007, coinciding with ADP1 measurements. The red dot represents the ADP-1 site location. The small lower panels show the time series of the wind used to force the model during that particular month, extracted at the center of Pegasus Bay. The stronger black wind vectors

emphasise the wind during two days prior to the flow snapshot, and the strong red vectors corresponds to the day of the flow snapshot.

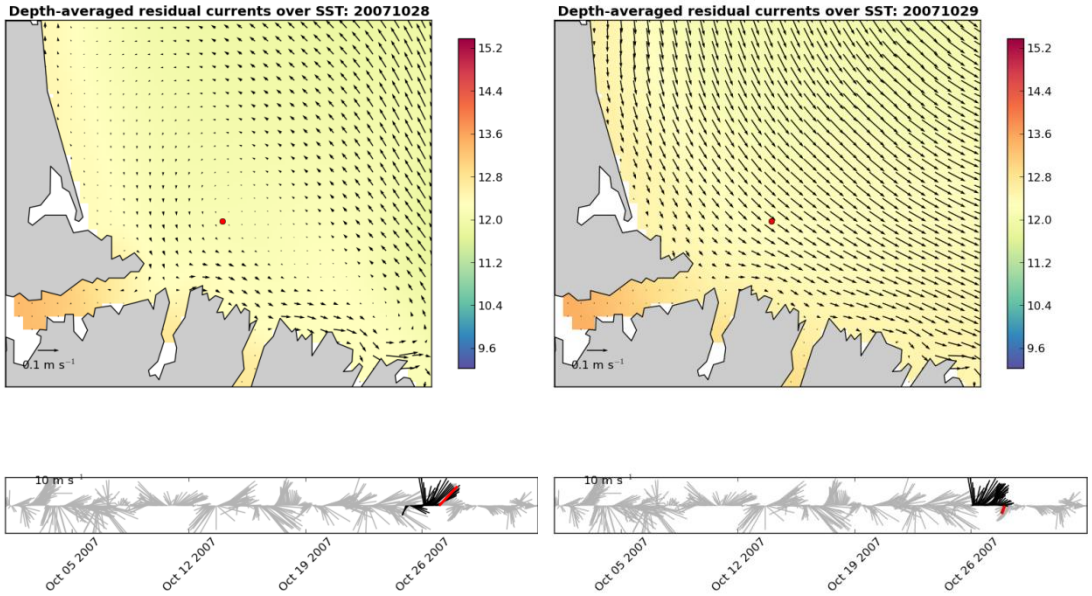

Figure 4.3 Zoom at the dump ground surroundings for PEGASUS ROMS domain residual depth-averaged flow daily snapshots for October 28 and 29, 2007, coinciding with ADP-1 measurements. The red dot represents the ADP-1 site location. The small lower panels show the time series of the wind used to force the model during that particular month, extracted at the center of Pegasus Bay. The stronger black wind vectors emphasise the wind during two days prior to the flow snapshot, and the strong red vectors corresponds to the day of the flow snapshot.

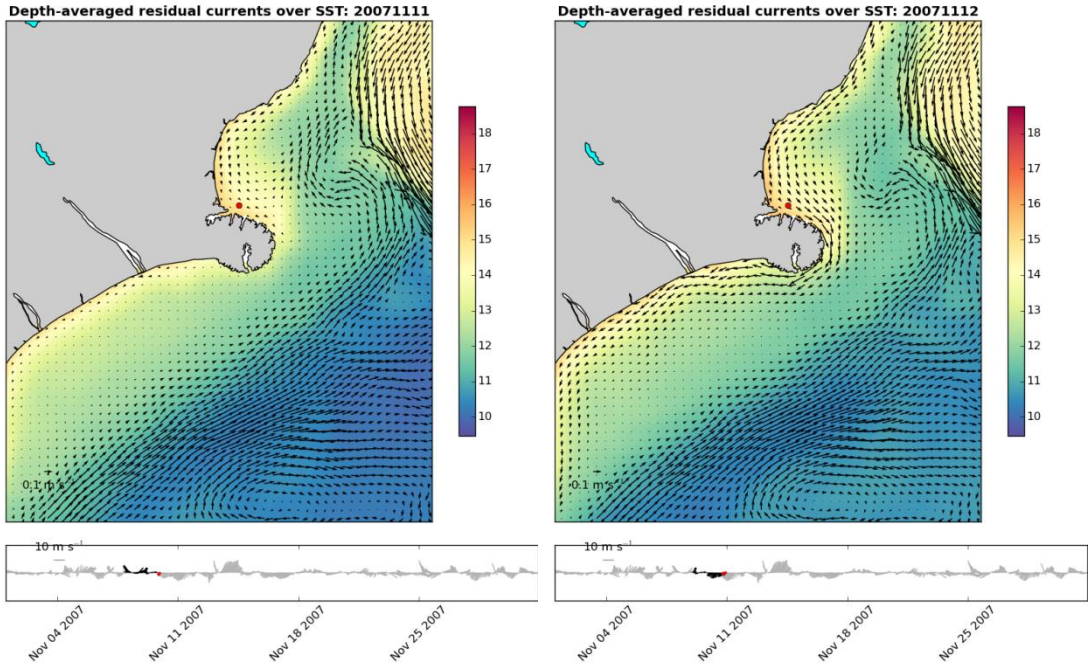

Figure 4.4 CESI ROMS domain residual depth-averaged flow daily snapshots for November 11 and 12, 2007, coinciding with ADP-1 measurements. The red dot represents the ADP-1 site location. The small lower panels show the time

series of the wind used to force the model during that particular month, extracted at the center of Pegasus Bay. The stronger black wind vectors emphasise the wind during two days prior to the flow snapshot, and the strong red vectors corresponds to the day of the flow snapshot.

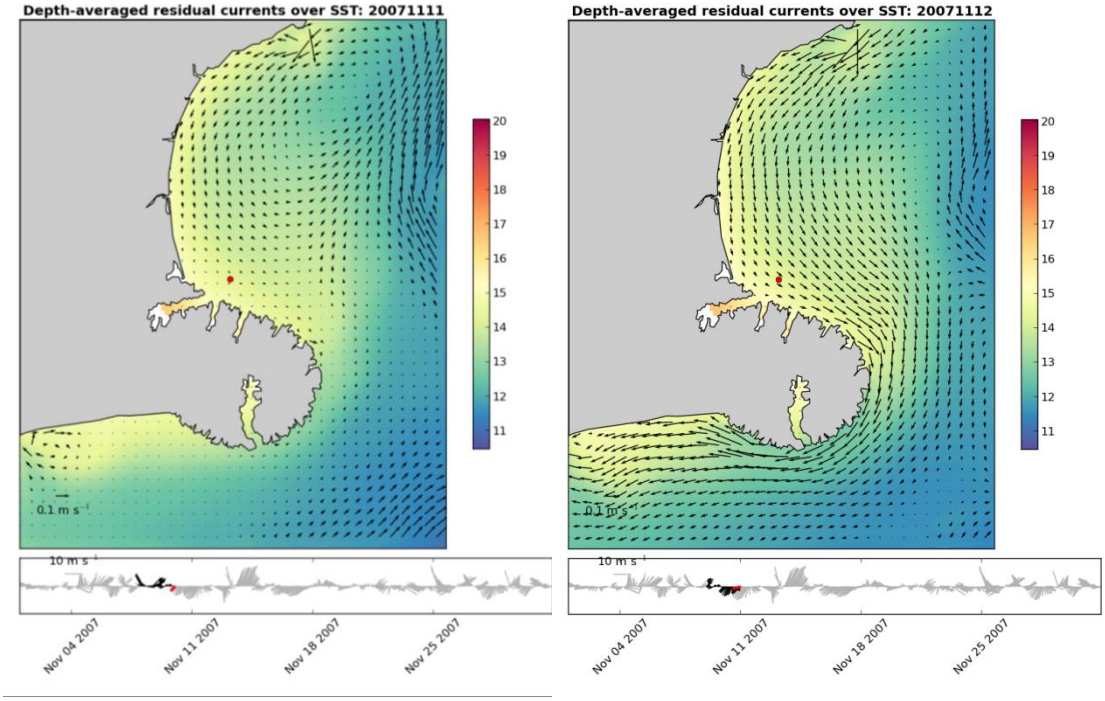

Figure 4.5 PEGASUS ROMS domain residual depth-averaged flow daily snapshots for November 11 and 12, 2007, coinciding with ADP-1 measurements. The red dot represents the ADP-1 site location. The small lower panels show the time series of the wind used to force the model during that particular month, extracted at the center of Pegasus Bay. The stronger black wind vectors emphasise the wind during two days prior to the flow snapshot, and the strong red vectors corresponds to the day of the flow snapshot.

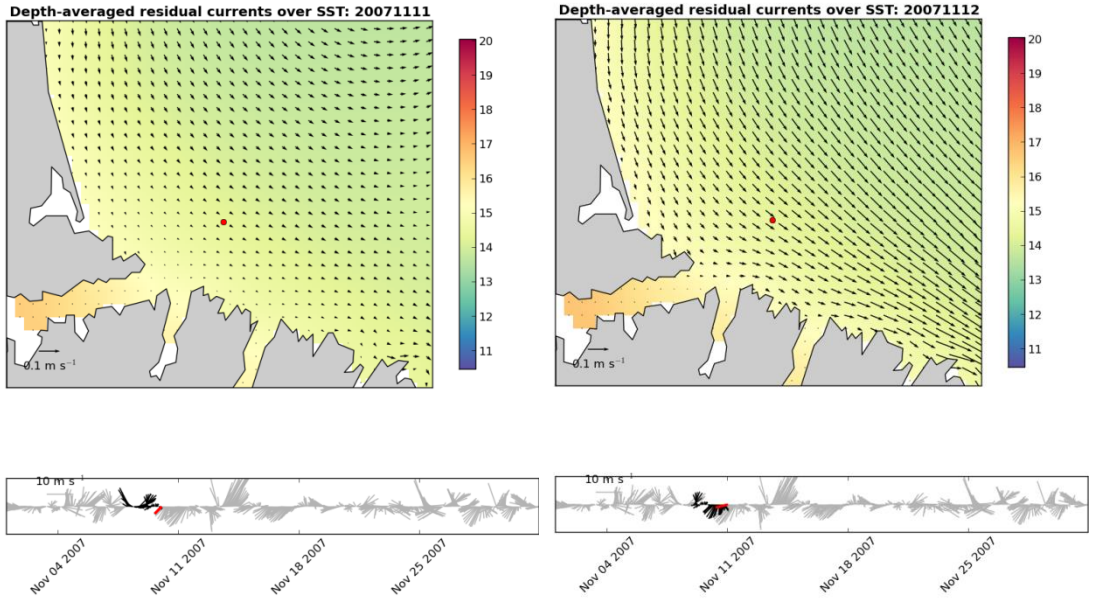

Figure 4.6 Zoom at the proposed dump ground surroundings for PEGASUS ROMS domain residual depth-averaged flow daily snapshots for November 11 and 12, 2007, coinciding with ADP-1 measurements. The red dot represents the ADP-1 site location. The small lower panels show the time series of the wind used to force the model during that particular month, extracted at the center of Pegasus Bay. The stronger black wind vectors emphasise the wind during two days prior to the flow snapshot, and the strong red vectors corresponds to the day of the flow snapshot.

5. CONCLUSION

A three-level downscaling approach with a 3D primitive equation hydrodynamic ocean model has been described and tested against field measurements. The purpose is to evaluate the model performance, accuracy and applicability to the scope described in Section 1. Primary focus is given to the sub-inertial (non-tidal) band of the circulation regime, which plays an important role in the dispersal of suspended sediments.

In general, the model shows good agreement for total velocities as well as for the residual currents. Tidal and residual currents have different predictability rates, the former being defined by a very well determined periodic oscillation provided, and the later dependent on a range of scales of motion caused by multiple local and remote forcing mechanisms that interact with each other are very difficult to predict in a real time basis without good data coverage combined with modern data assimilation techniques. However, the methodology used here is considered to fulfil the requirements to represent the physics of all the main hydrodynamic processes involved in this task, considering intensity and spatial-temporal variability of the flow environment impacting the area and the outcomes, bearing in mind the intrinsic cost-effectiveness of such a study.

The dominant flow regimes are successfully captured by the model with an acceptable degree of error. Overall underestimation by less than 2 $cm.s^{-1}$ was achieved in the vicinity of the proposed dump ground, and most of the significant flow events were capture by the model to an acceptable degree. It was noted that some significant flow events occurring in the measurements period were not captured by the model, as others were either under or over predicted.

Under prediction, over prediction or missing residual currents flow events is considered to be normal in the scientific literature in similar applications, as long as the model captures the essential flow regime and as long as no real-time prediction is required. This is one of the main reasons why forward hindcast approaches are conducted in very long term simulations, to overcome the ambiguities and assumptions related to punctual and short duration *in situ* measurements used as base for model validation. Once the model proved skill in simulating the dominant flow regime and the variability modes, long term runs are conducted to minimize the weakness of not being able to reproduce every single real time significant flow pattern. The long term simulation will include enough samples of events (some overestimated, some underestimated) to provide an appropriate basis for conclusion. One can always raise the question if the measurements were taken in a different site, in a different month, in a different season, etc. Slightly different results may arise from different details, as was noted here for two different campaigns.

The hydrodynamic modelling approach appears to have achieved a satisfactory result by combining the best of the two paradigms: observations and modelling. The valuable and costly measurements, sparse and punctual, were combined with a comprehensive numerical solution that evolves in time and space, to obtain the best ocean state estimation for the given purpose.

6. REFERENCES

Egbert, G.D., Erofeeva, S.Y., 2002. Efficient inverse modeling of barotropic ocean tides. J. Atmospheric Ocean. Technol. 19, 183–204.

Fairall, C. W., Bradley, E. F., Hare, J. E., Grachev, A. A., Edson, J. B., 2003. Bulk parameterization of air-sea fluxes: Updates and verification for the COARE algorithm. J. Clim. 16, 571–591.

Haidvogel, D.B, Arango, H.G., Budgell, W.P., Cornuelle, B.D., Curchitser, E., Di Lorenzo, E., Fennel, K., Geyer, W.R., Hermann, A.J., Lanerolle, L., Levin, J., McWilliams, J.C., Miller, A.J., Moore, A.M., Powell, T.M., Shchepetkin, A.F., Sherwood, C.R., Signell, R.P., Warner, J.C., Wilkin, J., 2008. Ocean forecasting in terrain-following coordinates: Formulation and skill assessment of the Regional Ocean Modeling System. J. Comput. Phys. 227, 3595–3624.

Saha, S., Moorthi, S., Pan, H.-L., Wu, X., Wang, J., Nadiga, S., Tripp, P., Kistler, R., Woollen, J., Behringer, D., Liu, H., Stokes, D., Grumbine, R., Gayno, G., Wang, J., Hou, Y.-T., Chuang, H.-Y., Juang, H.-M.H., Sela, J., Iredell, M., Treadon, R., Kleist, D., Van Delst, P., Keyser, D., Derber, J., Ek, M., Meng, J., Wei, H., Yang, R., Lord, S., Van Den Dool, H., Kumar, A., Wang, W., Long, C., Chelliah, M., Xue, Y., Huang, B., Schemm, J.-K., Ebisuzaki, W., Lin, R., Xie, P., Chen, M., Zhou, S., Higgins, W., Zou, C.-Z., Liu, Q., Chen, Y., Han, Y., Cucurull, L., Reynolds, R.W., Rutledge, G., Goldberg, M., 2010. The NCEP Climate Forecast System Reanalysis. Bull. Am. Meteorol. Soc. 91, 1015–1057. doi:10.1175/2010BAMS3001.1